1

INTRODUCTION

1.1 PHASE DIAGRAMS OF SINGLE FLUIDS

Substances appear in Nature in several states of aggregation: crystalline solids, amorphous solids, glasses, liquids, and gases. The latter two states are collectively termed "fluids" because they are subject to flow under moderate stresses (forces). A phase is a portion of space in which all the properties are homogeneous, that is, they do not depend on the precise location in the phase (except at its boundaries). Depending on the external conditions (thermodynamic states) of temperature and pressure, a substance may exist at several states of aggregation at the same time, each of which is represented as a different phase. These phases may be at equilibrium with each other, and the phase diagram, in terms of the external conditions of the temperature and pressure, represent which phases are at equilibrium with each other. These phase equilibria have several important features, governed by the phase rule of Gibbs. This rule states that number of degrees of freedom (*Df*) in a system is equal to 2 plus the number of components (*Co*) minus the number of phases that exist at equilibrium (*Ph*):

$$Df = 2 + Co - Ph \tag{1.1}$$

The degrees of freedom of interest in the present context are the external conditions that can be independently chosen: the pressure P, the temperature T,

Supercritical Water A Green Solvent: Properties and Uses, First Edition. Yizhak Marcus.

and the composition of mixtures. When the latter are expressed as the mole fractions of the components: $x_1, x_2, \ldots, x_N$ for an N-component mixture, there are $N-1$ independent composition variables. A component is a substance that can be added independently: water is an example of a component and a salt, such as NaCl, is another example, but each of their constituent ions (H^+ or H_3O^+, OH^-, Na^+, Cl^-) is not. Only neutral combinations of the ions can be considered as components, since they can be actually handled.

For a single substance $Co = 1$ and up to three phases can exist at equilibrium, in which case $Df = 0$, there remain no freely determinable external conditions (no degrees of freedom): the temperature and pressure are fixed. This invariant point (involving a solid, a liquid, and their vapor) is called the triple point of the substance. In the case of water: ice, liquid water, and water vapor are at equilibrium at 0.01°C ($T = 273.16$ K) and $P = 0.61166$ kPa [1].

Two phases of a single component at equilibrium permit according to the phase rule (1.1) a single degree of freedom: either the temperature is variable and the pressure is then fixed or for a variable pressure the temperature is fixed. This simple function determines a line in the two-dimensional phase diagram. For the water substance, at temperatures below freezing several phases of ice exist, depending on the pressure, and a pair of which can exist at equilibrium along the lines of the relevant phase diagrams. Ice may sublime to form water vapor, and again the two phases may exist at equilibrium along the sublimation line of the phase diagram of water. These aspects of the phase diagram of water are outside the scope of this book. The phase diagram of water is shown in Fig. 1.1, the phase boundaries being the coexistence lines of two phases at equilibrium. The phase diagram of water at very low temperatures and very high pressures is complicated by the existence of several ice phases of different densities and structures (not shown in Fig. 1.1), but these are of no concern in the present context.

When attention is drawn toward fluid phases, vapor–liquid equilibria (VLE) constitute a very important subject. Again, in such two-phase systems the feature of the phase diagram of water is a line, called the saturation line for VLE, and is designated by the subscript ($_\sigma$). This line for water is shown in Fig. 1.1, extending from the triple point up to the critical point (see below). The fact that the normal boiling point of water at ambient pressure (1 atm = 1.01325 bar = 101.325 kPa) happens to correspond to 100°C (373.15 K), is incidental in this respect. Wagner and Pruss reported the IAPWS 1995 formulation for the thermodynamic properties of ordinary water substance [1] that appears still to be the last word on the subject. The expression for the saturation vapor pressure $p_\sigma(T)$ takes the following form:

$$\ln(p_\sigma/P_c) = (1-\tau)^{-1}[a_1\tau + a_2\tau^{1.5} + a_3\tau^3 + a_4\tau^{3.5} + a_5\tau^4 + a_6\tau^{7.5}] \quad (1.2)$$

TABLE 1.1 Parameters for the Saturation Vapor Pressure of Water, Eq. (1.2)

P_c/MPa	T_c/K	a_1	a_2	a_3	a_4	a_5	a_6
22.064	647.096	−7.8595	1.84408	−11.78665	22.68074	−15.96187	1.801225

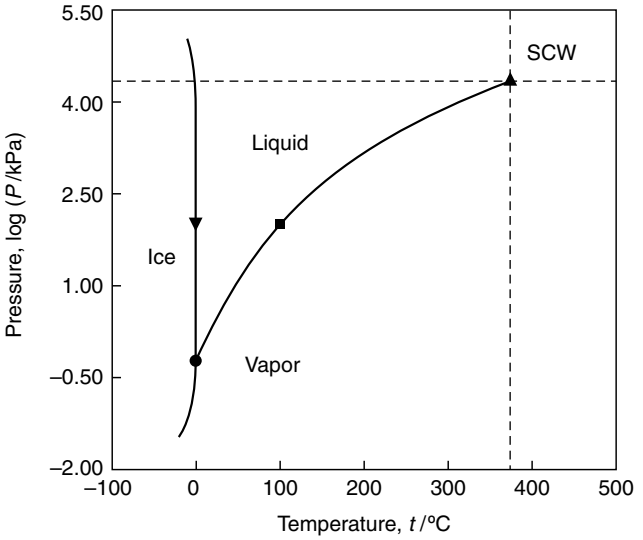

FIGURE 1.1 The phase diagram of water: point • corresponds to the triple point ($t_{tr} = 0.01°C$, $P_{tr} = 0.611$ kPa), point ▼ to the melting point ($t_m = 0°C$, $P_m = 101.3$ kPa), point ■ to the normal boiling point ($t_b = 100°C$, $P_b = 101.3$ kPa), and point ▲ to the critical ($t_c = 374°C$, $P_c = 22.1$ MPa). The line between • and ▲ is the saturation line, $P = p_\sigma$. Various compressed ices exist above point ▼ that are of no concern in the present context.

where P_c is the critical pressure and $\tau = 1 - T/T_c$, with T_c being the critical temperature. The values of P_c, T_c, and the coefficients a_i ($i = 1$–6) are shown in Table 1.1.

Numerical values of p_σ at several temperatures are shown in Table 1.5 along with data for other properties of liquid water discussed in Section 1.4.

A supercritical fluid (SCF) consists of a single phase and since $Co = Ph = 1$ it has two degrees of freedom according to Eq. (1.1). Its temperature and the pressure can be chosen at will, provided they are larger than the critical values (see below).

1.2 THE CRITICAL POINT

As the temperature and pressure of a fluid increase, a point is reached where the two phases, the liquid and the vapor, coalesce into a single phase.

The density of the liquid diminishes along the saturation line whereas that of the vapor increases as its pressure increases, until finally they become equal at the critical point. This is characterized by a critical temperature T_c, a critical pressure P_c, and a critical density ρ_c. A liquid that is confined in a vessel in a gravitational field has a free surface with respect to its vapor, hence, being denser, lies below it. However, at the critical point the meniscus that is characteristic of this surface disappears. Slightly below T_c the fluid becomes opalescent because of the fine dispersion of minute droplets of the liquid in the vapor of almost the same density. At temperatures and pressures above the critical ones, $T > T_c$ and $P > P_c$, the substance exists as a single clear phase, the supercritical fluid. According to the phase rule, Eq. (1.1), the supercritical fluid has two degrees of freedom, and the temperature and pressure can be chosen at will. These two external variables determine the properties of the supercritical fluid, such as its density, heat capacity, viscosity, relative permittivity, among many others, as are dealt with for the supercritical water (SCW) substance in Chapter 2. The critical temperature of water is $T_c = 647.096\,\mathrm{K} = 373.946^\circ\mathrm{C}$ and its critical pressure is $P_c = 22.064\,\mathrm{MPa} = 21.78\,\mathrm{atm}$ (cf. Tables 1.1 and 1.3). The critical density of water is $\rho_c = 322\,\mathrm{kg\,m^{-3}}$ and its critical molar volume is $V_c = 56.0 \times 10^{-6}\,\mathrm{m^3\,mol^{-1}}$, the latter two quantities being known to no better than $\pm 1\%$.

For many purposes, and especially for the description of the properties of supercritical fluids, it is expedient to use the reduced variables: the reduced temperature, $T_r = T/T_c$, the reduced pressure $P_r = P/P_c$, the reduced density $\rho_r = \rho/\rho_c$, or the reduced molar volume $V_r = V/V_c$. In the vicinity of the critical point there are some general relationships that depend on the deviation of the temperature from the critical point: $\tau = 1 - T_r$. As the critical point is approached from below ($\tau > 0$) the enthalpy of vaporization tends to zero and the heat capacity of the system tends to infinity according to the proportionality relationship

$$C_{\mathrm{P\ or\ V}} \propto \tau^{-\alpha} \tag{1.3}$$

The dependence of the density difference between the liquid and vapor phases on τ is according to Eq. (1.4):

$$\Delta\rho = \rho_{\mathrm{liq}} - \rho_{\mathrm{vap}} \propto \tau^{\beta} \tag{1.4}$$

The compressibility of either phase depends on the temperature as

$$\mathrm{d}\rho/\mathrm{d}P \propto \tau^{-\gamma} \tag{1.5}$$

At $\tau = 0$ (at the critical point) the reduced pressure depends on the reduced density as

$$P_r - 1 \propto (\rho_r - 1)^{\delta} \tag{1.6}$$

These proportionalities are described by means of the critical indices, the commonly accepted theoretical values for them being $\alpha \approx 0$, $\beta = 1/2$, $\gamma = 1$, and $\delta = 3$, assumed to be universal. However, for specific substances the values of these indices differ from the universal ones, as is the case for water (Section 1.5).

The densities of the liquid and vapor phases of a substance approach each other as the critical point is approached. The mean specific volume along the saturation curve is a linear function of the temperature, a nearly perfect experimental fact called the "law of rectilinear diameters":

$$[v_\sigma(\mathrm{l}) + v_\sigma(\mathrm{g})]/2 = a + bT \tag{1.7}$$

The value of the temperature coefficient b is generally small and negative, the a and b values for water are presented in Section 1.5.

1.3 SUPERCRITICAL FLUIDS AS SOLVENTS

Supercritical fluids have been proposed as solvents for many uses, both in the laboratory and industrially. Their properties as solvents are, therefore, of interest. The following comparison with gases and liquids (Table 1.2) are illuminating in this respect.

Supercritical fluids have an advantage over ordinary gaseous fluids for many applications in having much higher densities, and an advantage over ordinary liquids in having lower viscosities and considerable higher diffusivities. SCFs are well integrated in the modern tendency toward "green"

TABLE 1.2 Comparison of the Property Ranges of Supercritical Fluids with those of Gases and Liquids at Ambient Conditions

State	Density, ρ/kg m^{-3}	Viscosity, η/mPa s	Diffusivity, $10^6 D$/m^2 s^{-1}
Gases, ambient	0.6–2	0.01–0.03	10–40
SCFs, at T_c, P_c	200–500	0.01–0.03	~0.1
SCFs, at T_c, $4P_c$	400–900	0.03–0.09	~0.02
Liquids, ambient	500–1600	0.2–3	0.0002–0.002

TABLE 1.3 The Critical Points of Some Substances, Together with their Critical Densities, ρ_c

Substance	T_c/K	P_c/MPa	ρ_c/kg m^{-3}
Water, H_2O	647.096	22.064	322
Heavy water, D_2O	643.89	21.671	356
Carbon dioxide, CO_2	304.1	7.34	469
Methane, CH_4	190.4	4.60	162
Ammonia, NH_3	405.5	11.35	235
Ethene, C_2H_4	282.4	5.04	215
Ethane, C_2H_6	305.4	4.88	203
Methanol, CH_3OH	512.6	8.09	272
Ethanol, C_2H_5OH	513.9	6.14	276

solvents for reactions and separations that are ecologically friendly. They can be employed as reaction media, for extraction, separation, and purification, and for drug formulations, among other uses. In addition to being "green," they are tunable, so that their properties can be varied at will. The solvent power of supercritical fluids can be fine-tuned by adjustment of the temperature and pressure, hence of the density. This gives them some advantage over common solvents used at ambient conditions, although the solvent power of the latter can be tuned by mixing with cosolvents, as can also be done for SCFs, of course.

Table 1.3 reports the critical temperature, T_c, the critical pressure, P_c, and the critical density, ρ_c, of substances of interest in the present context.

The general mode of the application of SCFs is by dissolution of the reactants or the materials to be separated in them, carrying out the reaction and separation, and then recovering the products by either one of two techniques. One is by rapid diminution of the pressure, allowing the rapid expansion of the supercritical solvent (RESS technique) and eventual formation of the gaseous solvent (for recovery) leaving liquid or solid products behind. The other is the addition of an "antisolvent" that diminishes the solubility of the product in the SCF.

Following are some examples of the uses of SCFs as solvents.

- *Synthesis*: Diels–Alders reactions in supercritical water; polymerization of methyl methacrylate in supercritical difluoromethane; phase transfer catalysis by tetraheptylammonium bromide in supercritical carbon dioxide (SCD) modified with acetone.
- *Pyrolysis*: Conversion of biomass to fuel; complete oxidation of obnoxious materials in SCW (Chapter 5).
- *Separations*: Recovery of fat-soluble vitamins by SCD; delipidation of protein extracts; as chromatographic eluents in forensic analysis; fractionation of mono-, di- and triglycerides.

- *Small Particle Formulations*: Drug particle design, for example, for inhalable insulin; powder drying; microencapsulation.

An important issue for the use of SCFs is their solvent power. One way to describe this is in terms of the linear solvation energy relationship for a series of solutes in a given solvent or of a given solute in a series of solvents:

$$\log x_{\text{solute}} = p + q\rho_{\text{r}} + s\pi^*_{\text{solute}} + a\alpha_{\text{solute}} + b\beta_{\text{solute}} + vV_{\text{solute}} \tag{1.8}$$

Here x_{solute} is the mole fraction of the solute in the saturated solution, V_{solute} is its molar volume, and π^*_{solute}, α_{solute}, and β_{solute} are its Kamlet–Taft solvatochromic parameters, dealing with its polarity/polarizibility, hydrogen bond donation (or electron pair acceptance) ability, and hydrogen bond acceptance (or electron pair donation) ability [2]. The parameters p, q, s, a, b, and v characterize the SCF, the latter four depending on the reduced density, ρ_{r}. The parameter v is generally negative, solute solubilities decrease with increasing solute molar volumes. Some SCFs are apolar (e.g., SCD), that is, they are incapable of acceptance and donation of hydrogen bonds (or electron pairs), hence have $a = b = 0$ and their s values may be near zero or negative. Others are dipolar aprotic (like acetone) with $b = 0$ but have positive values for a and s, and still others are protic (like water and methanol) and have also $b > 0$, being capable of both acceptance and donation of hydrogen bonds.

Another way to describe the solvent power of an SCF is by means of its (Hildebrand) solubility parameter, δ_{H} [3]. For solute/solvent systems with small solute solubilities, the following expression

$$\ln x_{\text{solute}} = -V_{\text{solute}}(RT)^{-1}(\delta_{\text{H SCF}} - \delta_{\text{H solute}})^2 \tag{1.9}$$

is valid. Conformal fluids, that is, SCFs conformal with a reference fluid, generally interact through central forces of the van der Waals type. Their solubility parameter can be expressed by

$$\delta_{\text{H SCF}}/\text{MPa}^{1/2} = 2.15P_{\text{c}}^{1/2}T_{\text{r}}^{-1/4}\rho_{\text{r}} \tag{1.10}$$

They depend on the temperature and pressure mainly through the dependence of the reduced density, ρ_{r}. The solubility parameters of the solutes are available from group contributions and are assumed to be rather independent of the temperature and pressure for estimation of the solubility via Eq. (1.9). A difference $\delta_{\text{H SCF}} - \delta_{\text{H solute}} > 4\,\text{MPa}^{1/2}$ represents a low solubility of the solute. However, water is *not* a conformal fluid, since it interacts by dipole and

hydrogen bonding interactions beyond the van der Waals ones. Its solubility parameter is discussed in Section 2.6 and the resulting expression, Eq. (2.42), differs from Eq. (1.10).

The best-known and most widely employed supercritical fluid is SCD, used industrially on a large scale for the decaffeination of coffee. It has convenient T_c and P_c values: 30.9°C (304.1 K) and 72.4 atm (7.34 MPa), is environmentally friendly (its industrial contribution to the greenhouse gas inventory is negligible compared to that resulting from the burning of fossil fuels), is nonflammable, nontoxic (at low concentrations), and noncorrosive to common structural materials, and is cheap. Its main drawback is its low solvent power, the solubility of polar substances in it is rather small and even nonpolar substances are not very soluble in SCD. This situation can be ameliorated by the addition of modifiers, such as methanol, but a detailed discussion of SCD, its properties and uses, is outside the scope of this book.

Supercritical water has properties differing considerably from those of SCD; for some recent reviews, see Refs [4, 5]. Its critical (absolute) temperature is twice and its critical pressure almost three times those of SCD; its ranges of application are about 400–600°C and 30–100 MPa. Thus, although nontoxic, nonflammable, and environmentally friendly it involves certain technical difficulties in view of these high temperatures and pressures, and mainly also corrosion problems. Applications of SCW and problems involved with them are fully discussed in Chapter 5. Here the solvent powers are only mentioned, these being fully discussed in Chapter 4: SCW retains the hydrogen bond donation and acceptance abilities of the water molecule, and its relatively low permittivity permits dissolution of nonpolar solutes.

1.4 GASEOUS AND LIQUID WATER

Before going on to the properties of supercritical water, it is expedient to survey briefly the properties of water in the gas phase, as individual molecules and clusters, and in the liquid phase, in the latter case along the saturation curve (Fig. 1.1). Some of the properties of individual water molecules [6, 7], both H_2O and D_2O, are shown in Table 1.4. These properties are manifested when the water molecules are present at low pressures in the ideal gaseous state, where $PV/RT = 1$.

The nonideality of water vapor (gaseous water) at nonnegligible pressures can be expressed in terms of the compressibility factor Z and the virial expansion:

$$Z = PV/RT = 1 + B_2(T)V^{-1} + B_3(T)V^{-2} + \cdots \qquad (1.11)$$

TABLE 1.4 Some Molecular Properties of (Light) Water, H_2O and Heavy Water, D_2O

Property	H_2O	D_2O
Molar mass, $M/\mathrm{kg\,mol^{-1}}$	0.018015	0.020031
O−H(D) bond length, d/pm	95.72	95.75
H−O−H angle, °	104.523	104.474
Moment of inertia,[a] $I_A/10^{-30}\,\mathrm{kg\,m^{-2}}$	0.10220	0.18384
Moment of inertia,[a] $I_B/10^{-30}\,\mathrm{kg\,m^{-2}}$	0.19187	0.38340
Moment of inertia,[a] $I_C/10^{-30}\,\mathrm{kg\,m^{-2}}$	0.29376	0.56698
Hydrogen bond length, d/pm	276.5	276.6
Dipole moment, μ/D[b]	1.834	1.84
Electrical quadrupole moment, $\Theta/10^{-39}\,\mathrm{C\,m^2}$	1.87	
Polarizability, $\alpha/10^{-30}\,\mathrm{m^3}$	1.456	1.536
Collision diameter, σ/pm	274	
Potential energy minimum, $(u/k_B)/\mathrm{K}$	732	
O−H(D) bond energy at 0 K, $E/\mathrm{kJ\,mol^{-1}}$	44.77	
Proton (deuteron) affinity, $E/\mathrm{kJ\,mol^{-1}}$	762[c]	772[c]
Symmetrical stretching frequency, $\nu_1/\mathrm{cm^{-1}}$	3656.65	2671.46
Asymmetrical stretching frequency, $\nu_3/\mathrm{cm^{-1}}$	3755.79	2788.05
Bending frequency, $\nu_2/\mathrm{cm^{-1}}$	1594.59	1178.33
Zero point vibrational energy, $\mathrm{kJ\,mol^{-1}}$	55.31[d]	40.44[d]
Ideal gas heat capacity, $C_p^{ig}/\mathrm{J\cdot K^{-1}\cdot mol^{-1}}$	33.584	
Ideal gas entropy, $S^{ig}/\mathrm{J\,K^{-1}\,mol^{-1}}$	188.67	

[a] The moment of inertia I_A pertains to rotation round the O−H bond and I_B pertains to rotation round the axis through the oxygen atom, and I_C pertains to rotation round an axis perpendicular to the latter.
[b] $1\ \mathrm{D} = 3.33564 \times 10^{-30}\,\mathrm{C\,m}$.
[c] From Ref. [45].
[d] From Ref. [46].

The temperature-dependent B_i are called the second, third, and so on, virial coefficients. The experimental B_2 values from 50 to 460°C are expressed by [7]

$$B_2/\mathrm{cm^3\,mol^{-1}} = 37.15 - (5.1274 \times 10^4/(T/\mathrm{K}))\exp(1.7095 \times 10^5/(T/\mathrm{K})^2) \tag{1.12}$$

It is negative ($-1059\,\mathrm{cm^3\,mol^{-1}}$ at 20°C) but becomes less so as the temperature increases ($-292\,\mathrm{cm^3\,mol^{-1}}$ at 150°C and $-105\,\mathrm{cm^3\,mol^{-1}}$ at 325°C). Values of the third virial coefficient of water are less well known, B_3 is zero at <150°C, it is about $-5.9 \times 10^4\,\mathrm{cm^6\,mol^{-1}}$ at 150°C and changes sign near 300°C [8].

Water in the gaseous phase, unless at very low pressures, tends to associate to dimers, trimers, and larger clusters. The clustering to dimers and higher

oligomers can be regarded as an interpretation of the nonideality of the water vapor expressed by Eq. (1.11). Rowlinson [9] derived the equilibrium constant for the association of water molecules to dimers in terms of the partial pressures of the species as

$$\log(K_{\text{ass}}/\text{Pa}) = -3.644 + 1250/(T/\text{K}) \tag{1.13}$$

This corresponds to a (temperature independent) enthalpy of dimerization of $-23.9\,\text{kJ mol}^{-1}$ and would lead to the presence of a mole fraction of 0.04 for the dimers at the critical point [7]. Less negative enthalpies of dimerization were consistent with the speed of ultrasound, $-15.4 \pm 8.7\,\text{kJ mol}^{-1}$ [10] and values varying from $-16.3\,\text{kJ mol}^{-1}$ at 0°C down to $-11.4\,\text{kJ mol}^{-1}$ at the critical point were derived from computer simulations by Slanina [11]. However, a more recent estimate by Sit et al. [12] of the binding energy of the dimer is $-22.8\,\text{kJ mol}^{-1}$. A consequence of the uncertainty in the dimerization enthalpy is an uncertainty in the mole fraction of the dimer as pressure and density of the vapor (and the temperature) increase along the saturation line. The increased total pressure should enhance the dimerization, and mole fractions of $x_{\text{dim}} = 0.276$ and $x_{\text{trim}} = 0.006$ have been estimated by Slanina [13] for the dimer and trimer at the critical point.

The pressure dependence of the integrated infrared absorption intensities of the stretching modes $\nu_1 + \nu_3$ of water vapor ($3200–4200\,\text{cm}^{-1}$) at 300–450°C and up to 8 MPa is consistent with a low content of dimers. The resulting dimerization enthalpy $-16.7 \pm 3.8\,\text{kJ mol}^{-1}$ [14] is within the range of the values quoted above.

The Raman spectra of saturated water vapor were measured by Walrafen et al. [15], showing an isosbestic point at $3648.5\,\text{cm}^{-1}$ as the temperature is increased. Frequencies above this point are considered due to monomeric water, those below it, their intensities being proportional to the square of the density, are considered due to the dimers. A much higher mole fraction of dimers at the critical point results from the Raman data, namely $x_{\text{dim}} = 0.696$. This interpretation was subsequently withdrawn by the authors [16], since the resulting enthalpies of dimerization had the wrong sign. The two-species equilibrium suggested by the isosbestic point was attributed to low and high rotationally excited monomeric water molecules. This does not explain the proportionality of the low frequency Raman intensities to the square of the pressure (density), however.

Dimers are not considered to contribute appreciably to the infrared absorption of dilute water vapor in the atmosphere, whereas large clusters of, say, 30 molecules do [17]. These are of consequence to cloud formation and consist of multihydrated hydrogen and hydroxide ions: $H(H_2O)_n{}^+$ and $HO(H_2O)_m{}^-$, or even the neutral ion pairs or zwitterions $H^+(H_2O)_pOH^-$.

Clusters of water around other ions are found by mass spectrometry. A further consideration of these entities, important for cloud formation, is outside the scope of this book.

Turning now to liquid water along the saturation line, some of the relevant properties are collected in Table 1.5.

Several features of the property changes of the liquid water with increasing temperatures and diminishing densities, ρ, along the saturation line should be noted. The relative permittivity, ε_r, the dynamic viscosity, η, the surface tension, γ, and the molar enthalpy of vaporization, $\Delta_V H$, diminish steadily as the temperature is increased. On approaching the critical point, say above 300°C, they fall rather abruptly, the latter two quantities, γ and $\Delta_V H$ vanishing at the critical point. On the other hand, the constant pressure molar heat capacity, C_P, and the isothermal compressibility, κ_T, have a shallow minimum near 33 and 46°C, respectively, but increase with the temperature, diverging to infinity at the critical point.

Several derived quantities are of interest; for instance, the temperature and pressure derivatives of the relative permittivity have been reported by Fernandez et al. [18]. These yield according to Bradley and Pitzer [19] the limiting slopes for the Debye–Hückel theoretical expressions for the osmotic and activity coefficients and the apparent molar enthalpies and volumes of electrolytes in water up to 350°C along the saturation line as well at higher pressures. The complex permittivity of water was measured by Lyubimov and Nabokov [20, 21] up to 260°C along the saturation curve. The derived relaxation times decrease steadily from 5.82 ps at 40°C to 0.75 ps at 260°C. The corresponding values for heavy water, D_2O, are 25% to 12% larger.

Other derived quantities include the isobaric expansibility, α_P, or the pressure derivative of the compressibility itself (the second pressure derivative of the density), the isochoric (constant volume) molar heat capacity, C_V, and the speed of sound, u. These are to be found in the Steam Tables and they can be derived from the equation of state as presented most recently by Wagner and Pruss [1]. The internal pressure, $P_i = T\alpha_P/\kappa_T - p_\sigma$, has a maximum of 758 MPa near 172°C, diminishing to 473 MPa at 360°C. The cohesive energy density $(\Delta_V H^\circ - RT)/V$ decreases steadily from 2357 MPa at 0°C to 1653 MPa at 172°C to 236 MPa at 360°C. A liquid is deemed structured ("stiff") when the cohesive energy density is larger by $\geq$50 MPa than the internal pressure, as suggested by Marcus [22]. Since there is a crossover between these two dependencies by 328°C, liquid water above this temperature is no longer "stiff" according to this criterion.

An interesting derived quantity is the Kirkwood–Fröhlich dipole orientation parameter g, which reflects the association of the water molecules in the liquid. For a coordination number N_{co} (the number of nearest neighbors), obtainable experimentally from diffraction of X-rays or neutrons, g describes

TABLE 1.5 Some Properties of Liquid Water Along the Saturation Line

$t/°C$	p_σ/MPa	$\rho_\sigma/kg\,m^{-3}$	ε_r	$\eta/mPa\,s$	$\Delta_V H/kJ\,mol^{-1}$	$\gamma/mN\,m^{-1}$	$C_P/J\,K^{-1}\,mol^{-1}$	κ_T/GPa^{-1}	g	pK_W[a]
25	0.00317	997.05	78.46	0.890	44.04	71.96	75.29	0.4525	2.90	14.00
50	0.01235	988.00	69.90	0.547	43.09	67.93	75.31	0.4417	2.84	13.28
75	0.03856	974.82	62.24	0.374	42.24	63.54	75.53	0.4561	2.77	12.71
100	0.10133	958.36	55.41	0.282	41.50	58.78	75.95	0.4902	2.70	12.26
125	0.23203	939.05	49.36	0.218	39.2	53.79	76.70	0.549[b]	2.64	11.91
150	0.47574	917.04	43.94	0.182	38.1	48.70	77.63	0.634[b]	2.58	11.64
175	0.8926	894.5	39.16	0.143	36.7	43.28	78.92	0.745[b,c]	2.52	11.44
200	1.5551	865.86	34.74	0.134	35.0	37.81	80.75	0.883[b,c]	2.48	11.30
225	2.5505	834.3	30.80	0.118	32.8	32.03	83.44		2.45	11.22
250	3.9777	799.14	27.08	0.1062	30.5	36.18	87.36		2.38	11.20
275	5.949	741.0	23.63	0.0967	28.1	20.17	92.98		2.33	11.25
300	8.592	712.42	20.26	0.0859	25.3	14.39	100.87		2.25	11.38
325	12.058	649.0	15.84	0.0820	22.2	7.26	111.66		2.15	11.64
350	16.537	575.04	13.16	0.0659	16.0	3.79	126.10		2.00	12.14
373.95	22.064	317.76	5.44		0	0	∞		1.79	15.34[d]

Adapted from Refs [20, 49].
[a]From Ref. [23].
[b]From Ref. [47].
[c]Extrapolated with a quadratic fit to data at 0–150°C.
[d]From Ref. [48].

the average angle, θ_{ij}, between the dipoles of neighboring water molecules i and j:

$$g = 1 + N_{co}\langle \cos \theta_{ij} \rangle \tag{1.14}$$

The values of g are obtained from the measured relative permittivity according to

$$g = (9\varepsilon_0 k_B/N_A)(MT/\rho\mu^2)(\varepsilon_r - \varepsilon_\infty)(2\varepsilon_r + \varepsilon_\infty)/\varepsilon_r(\varepsilon_\infty + 2)^2 \tag{1.15}$$

Here ε_0, k_B, and N_A are the universal constants, M is the molar mass of water, ρ is its density (M/ρ is its molar volume, V), μ is its permanent dipole moment (Table 1.4), and ε_∞ is the infinite frequency permittivity, equal to the square of the infinite frequency refractive index, n_∞^2. The latter quantity is obtained from the polarizibility of water, α (Table 1.4) according to the Lorenz–Lorentz relation as

$$n_\infty^2 = (V + 2B\alpha)/(V - B\alpha) \tag{1.16}$$

where $B = 4\pi N_A/3$. The values of g, shown in Table 1.5, are calculated according to the polynomial reported by Marcus [22]. The g values >1 show that water is associated as a liquid, though to a diminishing extent as the temperature rises. The average angle, with an assumed (not much temperature dependent) coordination number $N_{co} = 4$, increases from 61.6° at 25°C to 78.3° at 200°C and 78.6° at the critical point, showing some alignment of the dipoles even at these high temperatures (an angle of 90° corresponds to no correlation between the dipoles and to no association).

The structuredness of water has been explored by the present author [22] in terms of several measures. One of these is the ratio of the difference of the standard molar Gibbs energies of condensation of light and heavy water to the difference in the hydrogen bond energies of these two kinds of water. The resulting average number of hydrogen bonds per water molecule diminishes from 1.34 at 5°C to 0.30 at 305°C, but there are several difficulties with this interpretation of the structuredness, as discussed in the cited paper. The heat capacity density of liquid water relative to its ideal gas is another measure of the structuredness. It changes only slightly, from 2.37 to 2.20 $J/K^{-1}\,cm^{-3}$ from 0 to 200°C, and remains considerably higher than for unstructured liquids, for which it is $\sim$0.6 $J/K^{-1}\,cm^{-3}$. The entropy deficit of liquid water relative to its vapor (corrected for association of the latter) and normalized with regards to this quantity for the unstructured methane, $\Delta\Delta_V S^\circ/R$, changes more from 8.35 at 0°C to 6.93 at 200°C and to 6.06 at 360°C, again being much larger than for unstructured liquids, for which it is 2.0. That is, water is

"ordered" according to this criterion. This measure of structuredness is quite well proportional to the dipole orientation parameter through the relevant temperature range: $(\Delta\Delta_V S^\circ/R)/g = 2.83 \pm 0.15$, both measures pertaining to the "order" in the liquid water [22].

Another quantity of interest is the ionic dissociation constant of the water, or rather the ion product $K_W = [H_3O^+][OH^-]$. The recent evaluation of Chen et al. [23] let to the values of pK_W (for K_W on the $(\text{mol kg}^{-1})^2$ scale) shown in Table 1.5. This reference provides also values for the enthalpy, entropy, heat capacity and volume changes for the ionization of water at its saturation pressure. Note that pK_W decreases (ionization increases) as the temperature increases up to ~250°C and increases again (ionization decreases) somewhat beyond this temperature.

Spectroscopic studies of liquid water along the saturation line reveal some interesting aspects. The overtone band of HOD shows features at 7000 and 7150 cm^{-1}, attributed by Luck [24] to nonhydrogen bonded water molecules, a band at 6850 cm^{-1} attributed to weakly cooperative hydrogen bonded molecules, and one at 6400 cm^{-1} attributed to strongly cooperative hydrogen bonded molecules. As expected, the latter diminish sharply from 52% at 0°C to 7% at 230°C and remain near that level up to 350°C. On the other hand, the nonhydrogen bonded molecules increase from ~10% at 0°C rather steadily to ~65% at 350°C. The ^{17}O NMR chemical shifts δ were measured by Tsukahara et al. [25] in pressurized water (30 MPa) from 25°C up to and beyond the critical point. The values of δ/ppm vary substantially linearly from −1 at 25°C to −18 at 350°C and the deduced extent of hydrogen bonding, relative to that in ambient water, η, is linear with it: $\eta = 1 + 0.0274(\delta/\text{ppm})$, thus diminishing to 0.51 at 350°C. The deduced reorientation relaxation times diminish sharply from 2.9 ps at 25°C to 0.6 ps at 100°C and then more gently to 0.1 ps at 350°C. These values may be compared with the dielectric relaxation times reported above.

Thermodynamic properties of heavy water, D_2O, along its saturation line have been reviewed and compared to those of light (ordinary) water, H_2O, by Hill and MacMillan [8] up to 325°C. The data shown are the liquid and vapor volumes (densities) and enthalpies and the specific heat of the liquid. Note that the critical point of D_2O is lower than that of H_2O by 3.21 K (Table 1.3).

As mentioned in Section 1.3, solvatochromic parameters can be used to predict the solubility of solutes in solvents according to Eq. (1.8). Lu et al. [26] reported plots of the Kamlet–Taft π^*, α and β solvatochromic parameters as well as those of Reichardt's $E_T(30)$ polarity index in water along the saturation line up to 275°C. One of these parameters, π^* that describes the polarity/polarizibility of the solvent, measured by means of the solvatochromic indicator 4-nitroanisole, is linear with the density of the water. Its temperature dependence curve is concave downward (π^* diminishing from 1.09 at

ambience to 0.69 at 275°C), whereas that of the hydrogen bond donation parameter α is concave upward (diminishing from 1.19 at ambience to 0.84 at 275°C). The hydrogen bond acceptance parameter β (for monomeric water) varies little up to 100°C, then increases by some 30% up to 150°C and remains more or less at this value up to 275°C. The polarity index $E_T(30)$ decreases linearly from 63 kcal mol^{-1} (264 kJ mol^{-1}) at ambience to 53 (222 kJ mol^{-1}) at 275°C. In pressurized (40 MPa) high temperature water [27] (up to 420°C, i.e., beyond the critical point), the values of π^* were again linear with the density of the water, $\pi^* = 1.77\rho - 0.71$ up to 360°C. If the pressure dependence of π^* for the liquid is assumed to be negligible, the result is $\pi^* = 0.980 + 7.12 \times 10^{-4}(t/°C) - 7.40 \times 10^{-6}(t/°C)^2$ for water along the saturation line. The alternative probes, 4-nitro- and 4-cyano-*N*,*N*-dimethylaniline yield values consistent with these for liquid water.

1.5 NEAR-CRITICAL WATER

There is no clear definition of "near-critical" water, but most publications tend to use this epithet for pressurized hot liquid water at temperatures $300 \leq t/°C \leq 375$. Near-critical water has been proposed as an environmentally benign medium for chemical reactions [28, 29], biomass decomposition [30] and gasification [31], or preparation of inorganic nanoparticles [32], to cite at random some recent applications.

As the critical point is approached the differences in properties between the liquid and the vapor diminish, the fluid becomes opalescent due to the minute dispersion of liquid-like and vapor-like domains, and the meniscus separating the liquid from the vapor vanishes at the critical point. There remaining no free surface at the critical point, the surface tension γ vanishes, and since no energy is needed to convert the liquid to its vapor (these states being identical) also the enthalpy of vaporization, $\Delta_V H$, vanishes and the heat capacities C_P and C_V diverge to infinity (Table 1.5). Still, the properties of water near the critical point, say within 1–5 K above and below it, have been studied intensively.

The law of rectilinear diameters, Eq. (1.7) applies to water as for other fluids. For water the values of the coefficients of the mean specific volumes are $a = (61.6 \pm 0.6) \times 10^{-3}\,m^3\,kg^{-1}$ and $b = (90.4 \pm 1.0) \times 10^{-6}\,m^3/kg^{-1} \cdot K^{-1}$ over a considerable range of temperatures: $T \geq 600$ K up to the critical point. The critical density derived from this expression is the accepted value of $322 \pm 3\,kg\,m^{-3}$.

The critical indexes (see Section 1.2) are supposed to have universal values, but when actual P, ρ, and T (PVT) data for water very near the critical point, at $\tau = 1 - T/T_c \sim 0.01$ are used somewhat different values result: $\alpha = 0.11$ (instead of ≈ 0), $\beta = 0.34$ (instead of 0.5), $\gamma = 1.21$ (instead of 1), and

$\delta = 4.56$ (instead of 3) [33]. A slightly different set was given earlier by Watson et al. [34]: $\alpha = 0.087$, $\beta = 0.335$, $\gamma = 1.212$, and $\delta = 4.46$. With these and 13 additional parameters the equation of state is established from $\tau = -0.002$ to 0.118 within the experimental errors of the *PVT* data. Also, the sound velocity u and heat capacity C_P data could be modeled well around the critical density. Considerably fewer parameters (only eight) are needed when the *PVT* data are modeled according to the three-site associated perturbed anisotropic chain theory (APACT), with a total mean deviation of ~1% for the density and ~2% for the pressure for $-0.27 \leq \tau \leq 1.97$ [35].

Supplementary values for $V(T, P)$ as well as the enthalpy and entropy of water at the near-critical region were reported by Kretzschmar et al. [36, 37], based on the industrial formulation of the IAPWS-97. These are of main interest for steam turbine calculations and need not be dealt with here.

The molar isochoric heat capacity (that at constant volume), C_V, was reported by Abdulagatov et al. [50] over the temperature range 140–420°C and at densities of 250–925 kg m^{-3}, encompassing the critical point, at which it diverges to infinity. More recently Abdulagatov et al. [51] drew the attention to the extrema of C_V. At the critical density of 322 kg m^{-3} and $\tau = -0.055$, $C_V = 63$ J/K^{-1} mol^{-1} and this value is reached again beyond the critical point at $\tau = 0.042$. In the two-phase region and at densities near the critical one C_V/J/K^{-1} mol^{-1} increases from 63 at $\tau = -0.055$ to 193 at $\tau = -0.039$ J/K^{-1} mol^{-1} to 234 J/K^{-1} mol^{-1} at $\tau = -0.0093$ [50].

The thermal conductivity of water shows a critical enhancement near the critical point [38] as does its viscosity, as discussed by Watson et al. [34]. The viscosity enhancement takes place in a region bounded by $|\tau| \leq 0.023$ and $|\rho_r - 1| \leq 0.25$ and a 22-parameter expression describes the viscosity of water both outside this interval (η'), and inside it, $\eta = \eta' + \Delta\eta$, including the enhancement, $\Delta\eta$. This depends on the density fluctuations near the critical point, described by the correlation length ξ, so that

$$\Delta\eta = \eta'(0.376\xi)^{0.054} - 1 \tag{1.17}$$

with ξ in nm. At 373.5°C and saturation pressure, the viscosity of liquid water is 47.02 μPa s and at 375°C and at 22.5 MPa (slightly above the critical point temperature and pressure, $t_c = 373.95$°C and $P_c = 22.06$ MPa) it is 41.79 μPa s, whereas in between it diverges to infinity [34].

The permittivity of water does not show a discontinuity near the critical point, it varies smoothly along the saturation curve and beyond the critical point [18]. On the other hand, the Raman scattering of the ν_1 stretching vibration of water shows according to Ikushima et al. [39] a moderate jump in the blue shift with increasing temperatures in the near-critical region as well a strong narrowing of the bandwidth. These changes are consistent with the

changes in the proton chemical shifts of the NMR spectrum measured by Matsubayashi et al. [40] that also show such jumps. The results were interpreted in a breakdown of the hydrogen bonded oligomeric structures in the near-critical region, leaving only hydrogen bonded dimers in addition to the monomers.

Turning now to heavy water, D_2O, and its mixtures with ordinary water, H_2O, the composition dependence of the critical temperature was measured by Marshall and Simonson [41] and is linear with the mole fraction of the former:

$$T_c/\mathrm{K} = 647.14 - 3.25 x_{D_2O} \tag{1.18}$$

The critical molar volumes of the two pure components, and presumably also of the HDO produced in the mixtures

$$D_2O + H_2O \leftrightarrows 2HDO \tag{1.19}$$

are the same, $56.0 \pm 0.1\ \mathrm{cm^3\ mol^{-1}}$. A crossover equation of state (see Section 2.1.3) was presented by Kiselev et al. [42] for D_2O and its mixtures with H_2O that fitted the data well also in the near-critical region. In a subsequent paper Bazaev et al. [43] refined the *PVT* data and Polikhronidi et al. [44] did the same for the isochoric heat capacity, C_V, for the equimolar mixture $D_2O + H_2O$ in the near-critical region.

1.6 SUMMARY

The phase diagram of a single pure substance reports the external conditions (temperature and pressure) at which two (or at most three) phases are at equilibrium with each other. The phase diagram of water is shown in Fig. 1.1. The vapor–liquid equilibrium line, showing the vapor pressure p_σ of water along the saturation curve is shown in Fig. 1.1 too, and is parametrized as Eq. (1.2) with parameters shown in Table 1.1. A supercritical fluid consists of a single phase and has two degrees of freedom, the temperature and the pressure can be chosen at will, provided they are larger than the critical values.

The critical point of fluids in general is discussed, the critical temperature of water being $T_c = 647.096\ \mathrm{K} = 373.946^\circ\mathrm{C}$ and its critical pressure is $P_c = 22.064\ \mathrm{MPa} = 21.78\ \mathrm{atm}$. The critical density of water is $\rho_c = 322\ \mathrm{kg\ m^{-3}}$ and its critical molar volume is $V_c = 56.0 \times 10^{-6}\ \mathrm{m^3\ mol^{-1}}$. The thermodynamic states of the supercritical fluids are often expressed in terms of the reduced quantities, that is, $T_r = T/T_c$, and so on. In the vicinity of the critical point there are some general relationships that depend on the deviation of the temperature from the critical point: $\tau = 1 - T_r$. The thermodynamic functions, such as the

heat capacity and compressibility, are then expressed in terms of the critical indices that are exponents of τ. The mean specific volume (of liquid + vapor) along the saturation curve is a linear function of the temperature, the "law of rectilinear diameters," Eq. (1.7), that extrapolates to the critical density.

Supercritical fluids have valuable properties that make some of them "green," that is, environmentally friendly solvents. An important property is their being tunable, the freely disposable pressure and temperature determine the density. Critical points of some useful SCFs are shown in Table 1.3 and the advantages of SCFs relative to liquids and gases are shown in Table 1.2. The solvent power of SCFs can be expressed in terms of the linear solvation energy relationship (1.8) or in terms of the solubility parameter expression (1.9). Some applications of SCFs are listed, but those of SCW are fully discussed in Chapter 5.

The properties of water below the critical point are dealt with for water vapor (gaseous water) and liquid water. At non-negligible pressures the pressure–volume–temperature (*PVT*) dependence of water vapor can be expressed in terms of the compressibility factor Z and the virial expansion (1.11). Clustering of water vapor molecules to dimers and higher oligomers can be regarded as an interpretation of the nonideality of the water vapor, Eq. (1.11). Uncertainty of the enthalpy of dimerization, as derived by several authors using different methods, for example, the partial pressure and the speed of ultrasound, leads to a great uncertainty of the extent of dimerization of the water vapor. The pressure dependence of the integrated infrared absorption intensities of the O−H bond stretching is consistent with a low content of dimers, but an interpretation of the corresponding dependence of the Raman scattering intensity yields an apparent large dimer content.

Some of the relevant properties of liquid water along the saturation line are collected in Table 1.5. The relative permittivity, ε_r, the dynamic viscosity, η, the surface tension, γ, and the molar enthalpy of vaporization, $\Delta_V H$, diminish steadily as the temperature is increased. On approaching the critical point, say above 300°C, they fall rather abruptly, the latter two quantities, γ and $\Delta_V H$ vanishing at the critical point, but the constant pressure molar heat capacity, C_P, and the isothermal compressibility, κ_T, increase with the temperature, diverging to infinity at the critical point. The ion product of water, $K_W = [H_3O^+][OH^-]$, describing its ionic dissociation along the saturation line, is shown in Table 1.5 as a function of the temperature.

Liquid water is deemed structured ("stiff") since its cohesive energy density is larger by $\geq$50 MPa than its internal pressure. However, there is a crossover between these two dependencies by 328°C, so that liquid water above this temperature is no longer "stiff" according to this criterion. The Kirkwood dipole orientation parameters g, Eq. (1.15), are shown in Table 1.5. The g values >1 show that water is associated as a liquid, though to a

diminishing extent as the temperature rises. The heat capacity density of liquid water relative to its ideal gas is another measure of the structuredness, being considerably higher than for unstructured liquids. The entropy deficit of liquid water relative to its vapor (corrected for association of the latter) and normalized with regards to this quantity for the unstructured methane is also much larger than for unstructured liquids, so that water is "ordered" according to these criteria. The extent of hydrogen bonding in liquid water can be derived from the difference in the Gibbs energies of condensation of light and heavy water and from the NMR chemical shifts of water. Both measures show a steady decrease as the temperature is raised, but this subject is more fully discussed in Section 3.4.

There is no clear definition of "near-critical" water, but most publications refer so to pressurized hot liquid water at temperatures $300 \leq t/°C \leq 375$. Near-critical water has been proposed as an environmentally benign ("green") medium. The solvatochromic parameters of water, relevant to Eq. (1.8), have been determined to 275°C, that is, still short of near-critical water. Values of the coefficients of the "law of rectilinear diameters," Eq. (1.7) and of the critical indices (exponents of τ, the distance from T_c) of near-critical water are presented in the text. The thermal conductivity and viscosity of water exhibit an enhancement in near-critical water, and detailed considerations of its isochoric heat capacity are also dealt with.

REFERENCES

1. W. Wagner and A. Pruss, *J. Phys. Chem. Ref. Data* **31**, 387 (2002).
2. S. Yalkowsky, *Aqueous Solubility: Methods of Estimation for Organic Compounds*, Marcel Dekker, New York, 1992.
3. Y. Marcus, *J. Supercrit. Fluids* **38**, 7 (2006).
4. M.-C. Bellisent-Funel, *J. Mol. Liq.* **90**, 313 (2001).
5. H. Weingärtner, *Angew. Chem. Intl. Ed.* **44**, 2673 (2005).
6. Y. Marcus, *The Properties of Solvents*, Wiley, Chichester, 1998.
7. D. Eisenberg and W. Kauzmann, *The Structure and Properties of Water*, Clarendon Press, Oxford, 1969.
8. P. G. Hill and R. D. C. Whalley, *J. Phys. Chem. Ref. Data* **9**, 735 (1980).
9. J. S. Rowlinson, *Trans. Faraday Soc.* **47**, 974 (1949).
10. R. A. Bolander and H. A. Gebbie, *Nature* **253**, 523 (1975).
11. Z. Slanina, *J. Mol. Struct.* **273**, 81 (1990).
12. P. L.-L. Sit and N. Marzari, *J. Chem. Phys.* **122**, 204510 (2005).
13. Z. Slanina, *Thermochim. Acta* **116**, 161 (1987).
14. G. V. Bondarenko and Yu. E. Gorbaty, *Mol. Phys.* **74**, 639 (1991).

15. G. E. Walrafen, W.-H. Yang, and Y. C. Chu, *J. Phys. Chem. B* **105**, 7155 (2001).
16. G. E. Walrafen, W.-H. Yang, and Y. C. Chu, *J. Phys. Chem. B* **103**, 1332 (2001).
17. H. R. Carlon, *J. Appl. Phys.* **52**, 3111 (1981).
18. D. P. Fernandez, A. R. H. Goodwin, E. W. Lemmon, J. M. H. Levelt Sengers, and R. C. Williams, *J. Phys. Chem. Ref. Data* **26**, 1125 (1997).
19. D. J. Bradley and K. S. Pitzer, *J. Phys. Chem.* **83**, 1599 (1979).
20. Yu. A. Lyubimov and O. A. Nabokov, *Russ. J. Phys. Chem.* **59**, 86 (1985).
21. O. A. Nabokov and Yu. A. Lyubimov, *Russ. J. Phys. Chem.* **61**, 106 (1987).
22. Y. Marcus, *J. Mol. Liquids* **79**, 151 (1999).
23. X. Chen, J. L. Oscarson, S. E. Gillespie, H. Cao, and R. M. Izatt, *J. Solution Chem.* **23**, 747 (1994).
24. W. A. P. Luck, *J. Mol. Struct.* **448**, 131 (1998).
25. T. Tsukahara, M. Harada, H. Tomiyasu, and Y. Ikeda, *J. Supercrit. Fluids* **26**, 73 (2003).
26. J. Lu, J. S. Brown, E. C. Boughner, C. L. Liotta, and C. A. Eckert, *Ind. Eng. Chem. Res.* **41**, 2835 (2002).
27. K. Minami, M. Mizuta, M. Suzuki, T. Aizawa, and K. Arai, *Phys. Chem. Chem. Phys.* **8**, 2257 (2006).
28. H. R. Patrick, K. Griffith, C. L. Liotta, C. A. Eckert, and R. Glaeser, *Ind. Eng. Chem. Res.* **40**, 6063 (2001).
29. Z. Dai, B. Hatano, and H. Tagaya, *Appl. Catal. A. Gen.* **258**, 189 (2004).
30. A. Sinag, S. Gűlbay, B. Uskan, and M. Canel, *Energy Conv. Manag.* **51**, 612 (2010).
31. P. Azadi, K. M. Syed, and R. Farnood, *Appl. Catal. A. Gen.* **358**, 65 (2009).
32. P. Hald, M. Bremholm, S. B. Iversen, and B. B. Iversen, *J. Solid State Chem.* **181**, 2681 (2008).
33. M. A. Anisimov, S. B. Kiselev, and I. G. Kostyukova, *Teplof. Vysok. Temp.* **25**, 31 (1987).
34. J. T. R. Watson, R. S. Basu, and J. V. Sengers, *J. Phys. Chem. Ref. Data* **9**, 1255 (1980).
35. P. J. Smits, I. G. Economou, C. J. Peters, and J. de S. Arons, *J. Phys. Chem.* **98**, 12080 (1994).
36. H.-J. Kretzschmar, I. Stocker, T. Willkommen, J. Trubenach, and A. Dittmann,in P. R. Tremaine,Ed., *Steam, Water, and Hydrothermal Systems: Physics and Chemistry Meeting the Needs of Industry*, National Research Council Canada, Ottawa, 2000, p. 255.
37. H.-J. Kretzschmar, J. R. Cooper, J. S. Gallagher, A. H. Harvey, K. Knobloch, R. Mares, K. Miyagawa, N. Okita, R. Span, I. Stocker, W. Wagner, and I. Weber, *J. Eng. Gas Turb. Power* **129**, 294, 1125 (2007).
38. R. S. Basu and J. V. Sengers,in A. Cezairlian,Ed., *Proceedings of the 7th Symposium on Thermophysical Properties*, American Society of Mechanical Engineers, New York, 1977, p. 822.

39. Y. Ikushima, K. Hatakeda, N. Saito, and M. Arai, *J. Chem. Phys.* **108**, 5855 (1998).
40. N. Matsubayashi, C. Wakai, and M. Nakahara, *J. Chem. Phys.* **107**, 9133 (1997).
41. W. L. Marshall and J. M. Simonson, *J. Chem. Thermodyn.* **23**, 613 (1991).
42. S. B. Kiselev, A. M. Abdulagatov, and A. H. Harvey, *Int. J. Thermophys.* **20**, 563 (1999).
43. A. R. Bazaev, I. M. Abdulagatov, J. W. Magee, E. A. Bazaev, and A. E. Ramazanova, *J. Supercrit. Fluids* **26**, 115 (2003).
44. N. G. Polykhronidi, I. M. Abdulagatov, J. W. Magee, and G. V. Stepanov, *Int. J. Thermophys.* **24**, 405 (2003).
45. M. DePaz, J. J. Leventhal, and L. Friedman, *J. Chem. Phys.* **51**, 3748 (1969).
46. C. Dekerckheer, O. Dahlem, and J. Reisse, *Ultrason. Sonochem.* **4**, 205 (1997).
47. G. S. Kell and E. Whalley, *J. Chem. Phys.* **62**, 3496 (1975).
48. J. C. Tanger, Jr. and K. S. Pitzer, *AIChE J*. **35**, 1631 (1989).
49. Y. Marcus, *Ion Solvation*, Wiley, Chichester, 1985.
50. I. M. Abdulagatov, V. I. Dvoryanchikov, and A. N. Kamelov, *J. Chem. Eng. Data*, **43**, 830 (1998).
51. A. I. Abdulagatov, G. V. Stepanov, I. M. Abdulagatov, A. E. Ramazanova, and G. S. Alisultanova, *Chem. Eng. Commun.* **190**, 1499 (2003).